Population-based Correspondence Models for Respiratory Motion Estimation in the Presence of Inter-fraction Motion Variations

Matthias Wilms[1], René Werner[2], Tokihiro Yamamoto[3], Heinz Handels[1], and Jan Ehrhardt[1]

[1]Institute of Medical Informatics, University of Lübeck, Lübeck, Germany
[2] Department of Computational Neuroscience, University Medical Center Hamburg-Eppendorf, Hamburg, Germany
[3] Department of Radiation Oncology, University of California Davis, Sacramento, USA
wilms@imi.uni-luebeck.de

Abstract. Many respiratory motion compensation approaches in radiation therapy of thoracic and abdominal tumors are guided by external breathing signals. Patient-specific correspondence models based on planning 4D data are used to relate signal measurements to internal motion. The motion estimation accuracy of these models during a treatment fraction depends on the degree of inter-fraction motion variations. Here, we investigate whether motion estimation accuracy in the presence of inter-fraction motion variations can be improved by (sub)population models, which incorporate patient-specific motion information and motion data from selected additional patients. A sparse manifold clustering approach is integrated into a regression-based correspondence modeling framework for automated identification of subpopulations of patients with similar motion characteristics. In an evaluation with repeated 4D CT scans of 13 patients, subpopulation models, on average, outperform patient-specific correspondence models in the presence of inter-fraction motion variations.

1 Introduction

Respiratory motion is a key problem in external beam radiation therapy (RT) of thoracic and abdominal tumors. In clinical practice, this problem is typically tackled by the use of technical motion compensation approaches (e.g., gating or tumor tracking) [1]. Most compensation approaches are guided by (external) breathing/surrogate signals (e.g., spirometry, skin surface displacements). Given a signal measurement, a trained correspondence model, which relates signal measurements to internal motion patterns, can be used to estimate the complex 3D motion of internal structures during the treatment [2].

Several approaches for correspondence modeling and model-based respiratory motion estimation in RT in general have been proposed over the past decade (see [2] and [3] for overviews). From a methodological point of view, most approaches

are either patient-specific or population-based. Patient-specific correspondence models [4–6] are built prior to the treatment based on planning 4D CT/MRI data of the specific patient. In contrast, (inter-patient) population-based models are build from motion data of several patients and typically model the mean motion (+ deviations from the mean) [7, 8]. Population models can, e.g., be adapted to unseen patients to allow for model-based motion estimation in the absence of patient-specific 4D planning data.

In most population-based approaches, the complete population is used to compute the model. Hence, the possible existence of subpopulations that optimally resemble the unseen patient's true motion is ignored. Recently, approaches for selecting/determining subpopulations of patients with motion patterns most similar to those of the unseen patient have been proposed [9–12].

Despite these developments, most of the time patient-specific models still outperform population models. However, the accuracy of a patient-specific correspondence model built on planning data and applied during a treatment fraction highly depends on the degree of inter-fraction motion variations [6]. We hypothesize that a patient's inter-fraction motion variability resembles the inter-patient motion variations observed in a subpopulation of patients with similar breathing characteristics. In this work, we, therefore, investigate whether the motion estimation accuracy in the presence of inter-fraction motion variations can be improved by correspondence models, which incorporate both, patient-specific motion information obtained from a planning data set as well as motion information from selected additional patients. To automatically identify subpopulations of patients with similar motion characteristics, we propose using a sparse manifold clustering approach, which is integrated into a regression-based correspondence modeling framework. The proposed approach is evaluated by means of repeated 4D CT scans of 13 lung cancer patients.

2 Methods

The goal of our approach is to build a correspondence model for a patient $p = 0$ with available planning data acquired prior to the treatment. We assume the planning data of this patient to consist of a 4D CT data set $(I_{0,j})_{j=1}^{n_{ph}}$ with n_{ph} 3D images $I_{0,j} : \Omega_0 \to \mathbb{R}$ ($\Omega_0 \subset \mathbb{R}^3$) capturing the patient's anatomy at breathing phases j and corresponding n_{sur}-dimensional surrogate signal measurements $(\zeta_{0,j})_{j=1}^{n_{ph}}$ with $\zeta_{0,j} \in \mathbb{R}^{n_{sur}}$. We furthermore assume a population of n_{pat} other patients to be given. The data available for each of these population patients $p \in \{1, \ldots, n_{pat}\}$ also consists of a 4D CT image sequence $(I_{p,j})_{j=1}^{n_{ph}}$ with $I_{p,j} : \Omega_p \to \mathbb{R}$ and n_{ph} corresponding surrogate signal measurements $\zeta_{p,j} \in \mathbb{R}^{n_{sur}}$. For the sake of simplicity, we assume temporal correspondence between the phases j across all patients.

After explaining the preprocessing of the data (Sec. 2.1), we will briefly review our patient-specific correspondence modeling approach (Sec. 2.2), before a general population-based extension (Sec. 2.3) and the new subpopulation-based approach (Sec. 2.4) are presented.

2.1 Preprocessing

As a first step, the 4D images sequences of all patients are mapped to a common atlas space Ω_A to establish anatomical correspondence between all data sets. The atlas space is generated following the approach presented in [13] by using the population patients. After this preprocessing, the reference breathing phases $j = 1$ (here: end-inspiration) of all patients are anatomically aligned, while breathing-related anatomical differences between patients in other phases are preserved. Please note, that the surrogate signals need to be transformed accordingly.

2.2 Patient-specific correspondence modeling

Our patient-specific correspondence modeling approach [4] is based on the assumption that a linear relation between a surrogate signal measurement $\hat{\zeta}_0$ and the corresponding internal motion $\hat{\varphi}_0$ exists. The non-linear transformation $\hat{\varphi}_0 = id + \hat{u}_0 : \Omega_A \rightarrow \Omega_A$ represents the deformation of the internal structures between the reference phase $I_{0,1}$ and the breathing state represented by $\hat{\varphi}_0$. Here, $\hat{u}_0$ denotes a displacement field. Mathematically, we define the relationship between $\hat{\zeta}_0$ and $\hat{\varphi}_0/\hat{u}_0$ as

$$\hat{\mathbf{u}}_0 = \overline{\mathbf{u}} + \mathbf{B}\hat{\zeta}_0 \ , \tag{1}$$

where $\hat{\mathbf{u}}_0 \in \mathbb{R}^{3m}$ (m: number of image voxels) denotes a vector containing all elements of the displacement field $\hat{u}_0$, $\mathbf{B} \in \mathbb{R}^{3m \times n_{sur}}$ is a coefficient matrix, and $\overline{\mathbf{u}} \in \mathbb{R}^{3m}$ is the mean displacement vector.

Model training consists of learning the coefficient matrix $\mathbf{B}$ (and calculating $\overline{\mathbf{u}}$) in Eq. (1). First, internal motion data is derived from the planning data by estimating non-linear transformations $(\varphi_{0,j})_{j=1}^{n_{ph}}$ between the reference phase $I_{0,1}$ and each $I_{0,j}$ via image registration [14]. Subsequently, least squares regression is performed based on the vectorized displacements fields $(\mathbf{u}_{0,j})_{j=1}^{n_{ph}}$ of the estimated transformations and the corresponding surrogate signal measurements $(\zeta_{0,j})_{j=1}^{n_{ph}}$ to obtain $\mathbf{B}$. See [4] for further details. This model represents the breathing characteristics captured by the patient-specific planning data.

2.3 Population-based correspondence modeling

The patient-specific correspondence model built in Sec. 2.2 is extended to a general population-based model by adding internal motion information and corresponding surrogate signal measurements from all n_{pat} population patients to the training data used to estimate coeffcient matrix $\mathbf{B}$ in Eq. 1. Therefore, non-linear transformations $(\varphi_{p,j})_{j=1}^{n_{ph}}$ between the reference phase $I_{p,1}$ and all other images $I_{p,j}$ of each patient p have to be computed. Finally, the training data consists of displacement fields $(\mathbf{u}_{p,j})_{p=0,j=1}^{n_{pat},n_{ph}}$ and corresponding surrogate signal measurements $(\zeta_{p,j})_{p=0,j=1}^{n_{pat},n_{ph}}$.

As all patients are represented by the same number of samples in the training data and no weighting is applied, least-squares regression averages out differences between patients. Hence, the influence of the patient-specific planning data of patient $p = 0$ depends on the population size.

2.4 Subpopulation-based correspondence modeling

As stated before, we hypothesize that a patient's inter-fraction motion variability resembles the inter-patient motion variations observed in a (sub)population of patients with similar breathing characteristics. The general population model in Sec. 2.3 is built based on data from all population patients, which might lead to an improved estimation accuracy. However, we assume that most of the time the heterogeneity of the population/large inter-patient differences will negatively impact the accuracy. We are therefore interested in identifying a subset $S \subseteq \{1, \ldots, n_{pat}\}$ of population patients with breathing characteristics most similar to that of the unseen patient $p = 0$ to build a more accurate model.

Our idea is to determine subset S by clustering the motion of all patients with respect to their similarity. In the end, the cluster the new patient $p = 0$ belongs to is chosen as S. Motion clustering has also been used by Peressutti *et al.* [11] to identify patients with similar breathing characteristics to personalize affine population models for cardiac respiratory motion compensation. However, in our application we have to deal with non-linear deformations and, furthermore, our clustering approach based on sparse coding is more general than the one used in [11] as it is able to effectivly handle high-dimensional data with complex structure.

Motion representation We start by representing the motion of each patient $p \in \{0, \ldots, n_{pat}\}$ by a vector $\mathbf{m}_p = [\mathbf{u}_{p,EE}^T, \mathbf{u}_{p,MI}^T, \mathbf{u}_{p,ME}^T]^T \in \mathrm{R}^{9m}$. Each vector $\mathbf{m}_p$ consists of a concatenation of three selected displacement field vectors $\mathbf{u}_{p,j}$, which encode the motion between the reference phase EI (end-inspiration) and the phases of end-expiration ($j = EE$), mid-inspiration ($j = MI$), and mid-expiration ($j = ME$) extracted from the 4D CT data sets (cf. Sec. 2.3). While the motion between EI and EE serves as a general representative for the motion of patient p, hysteresis-related patterns are captured by integration of the motion between EI and MI/ME.

Motion clustering We now assume that these vectors $\mathbf{m}_p$ lie in or close to multiple low-dimensional manifolds embedded in the high-dimenional ambient space. A (spectral) clustering solely based on pairwise distances computed in the ambient space might ignore this (possible) structure and assign motion vectors belonging to different manifolds to the same cluster. In order to avoid this, we employ the Sparse Manifold Clustering and Embedding (SMCE) method [15]. The approach aims to find a small number of neighbors $\{\mathbf{m}_i\}_{i \neq p}$ of each data point/motion vector $\mathbf{m}_p$ that belong to the same manifold and, therefore, approximately span a low-dimensional affine subspace passing near $\mathbf{m}_p$. An advantage of SMCE over other approaches is that these neighbors are automatically found, without the manual selection of a neighborhood radius or a fix neighborhood size.

Next, for each motion vector $\mathbf{m}_p$ a sparse weighting vector $\mathbf{w}_p \in \mathbb{R}^{n_{pat}+1}$ is computed whose non-zero elements indicate the (inverse) distances of the selected neighbors of $\mathbf{m}_p$ to $\mathbf{m}_p$. From these vectors $\{\mathbf{w}_p\}$, a similarity matrix

$$\mathbf{W} = \left[|\mathbf{w}_0| \ \ldots \ |\mathbf{w}_{n_{pat}}| \right] \tag{2}$$

is build, which is subsequently used for k-means-based spectral clustering [16]. Here, k denotes the number of clusters to be obtained. This parameter should be chosen with respect to the low-dimensional structure of the high-dimensional data ($k \geq$ # of manifolds).

Finally, the subpopulation of patients (including $p = 0$) specified by motion vectors belonging to the same cluster as $\mathbf{m}_0$ are used to generate a subpopulation model following the steps outlined in Sec. 2.3.

2.5 Experiments

An evaluation of the different models presented in Sec. 2.2–2.4 in the presence of inter-fraction variations of respiratory lung motion is carried out on repeated 4D CT data sets (10 breathing phases; resampled to a spatial resolution of $2.5 \times 2.5 \times 2.5\,\text{mm}$) of 13 lung cancer patients (see [17] for details). For each of these 13 patients, 2 4D CT data sets acquired at different days (Day1 and Day2) are available. 20 4D CT data sets of different patients are additionally used as population patients. In total, 46 4D CT data sets are used for the experiments.

During preprocessing (cf. Sec. 2.1), intra-patient/intra-fraction registrations restricted to the lungs are performed to estimate the respiratory lung motion of all patients in atlas space. The resulting transformations are used to build different models and serve as ground-truth motion data for evaluation. Model-based estimation accuracy is quantitatively evaluated by computing mean vector differences between a displacement field $\hat{u}_j$ estimated by a correspondence model and the ground-truth field u_j computed via registration for all inner-lung voxels. Due to the lack of available real surrogate data for the data sets used, a $n_{sur} = 2$-dimensional spirometry signal (signal value + time derivative) is simulated by an image-based analysis of the air content inside the lungs (see [4] for details).

For each of the 26 4D CT data sets of the different day cohort (13 patients with 2 repeated scans), 4 different correspondence models are built: (1) a patient-specific intra-fraction model, (2) a patient-specific inter-fraction model, (3) a population model, and (4) a subpopulation model. Each model is used to estimate the lung motion between the reference phase EI and the phases at MI, ME, and EE in the experiment-specific test data set.

Patient-specific intra-fraction model To establish a reference for performance comparison, a patient-specific intra-fraction model (cf. Sec. 2.2, [4]) is built for each data set by using a leave-out strategy. Phases at MI, ME, and EE are left out during training, respectively, and the motion between the reference phase EI and the left-out phases is estimated by the trained correspondence model.

Patient-specific inter-fraction models Patient-specific inter-fraction models (cf. Sec. 2.2) are built based on the internal motion data and the surrogate signal of the Day1 (Day2) data set to perform a model-based estimation of the motion in the Day2 (Day1) data set. Results of these models will give an impression on how well a patient-specific correspondence model build on pre-treatment planning data is able to estimate motion during a treatment fraction at a different day.

Table 1. Mean estimation errors obtained for the surrogate-based estimation of inner lung motion for the different correspondence models, given as mean±standard deviation per phase for the 26 data sets considered. Last column: mean results over all 3 phases.

	Mean estimation error [mm]			
Motion estimation	**EI → EE**	**EI → MI**	**EI → ME**	**Mean**
No motion estimation	8.59 ± 3.92	4.80 ± 2.27	7.09 ± 3.36	6.83 ± 3.58
Inter-fraction motion difference	4.06 ± 1.48	3.17 ± 0.85	3.62 ± 1.36	3.62 ± 1.30
Models:				
Patient-specific intra-fraction	1.45 ± 0.70	2.19 ± 1.02	1.47 ± 0.73	1.71 ± 0.89
Patient-specific inter-fraction	3.75 ± 1.31	2.91 ± 1.04	3.34 ± 1.14	3.34 ± 1.20
Population model	4.52 ± 1.56	2.87 ± 0.91	4.06 ± 2.08	3.82 ± 1.72
Subpopulation model	3.33 ± 0.99	2.59 ± 0.85	3.01 ± 0.93	2.97 ± 0.96

Population model For each data set, a population model (cf. Sec. 2.3) is built using a population of $n_{pat} = 44$ data sets (both data sets of the remaining 12 patients with repeated data + 20 patients with single session data) and the Day1 (Day2) data set of the specific patient. Each model is used to estimate the lung motion in the corresponding Day2 (Day1) data set.

Subpopulation model For each data set, a subpopulation model (cf. Sec. 2.4) is built using the same population as for the population models. However, a spectral motion clustering based on the Day1 (Day2) data set is carried out as described in Sec. 2.4 to identify a suitable subpopulation of patients. The $k-$means algorithm is run with $k = \{2, \ldots, 44\}$ clusters. In this work, k is retrospectively optimized for each patient with respect to the estimation error. Resulting models are used for motion estimation in the Day2 (Day1) data sets.

3 Results

Quantitative results of our evaluation are listed in Tab. 1. As expected, patient-specific intra-fraction models are giving (by far) the best results in terms of estimation accuracy. For the experiments where the motion in the different day data sets has to be estimated, the patient-specific inter-fraction models have on average a significantly higher estimation accuracy than the general population models (paired t-test; $p < 0.05$). This result supports our hypothesis that the heterogeneity of the population negatively impacts the accuracy of general population models. In contrast, the results of the subpopulation models show, on average, a significant improvement in terms of estimation accuracy compared to the results of the patient-specific inter-fraction models ($p < 0.01$). For some patients with large inter-fraction motion differences, mean improvements $>$ 1mm are achieved by using the subpopulation models instead of the patient-specific inter-fraction models (see Fig. 1). On average, 7.77 ± 10.18 patients were used

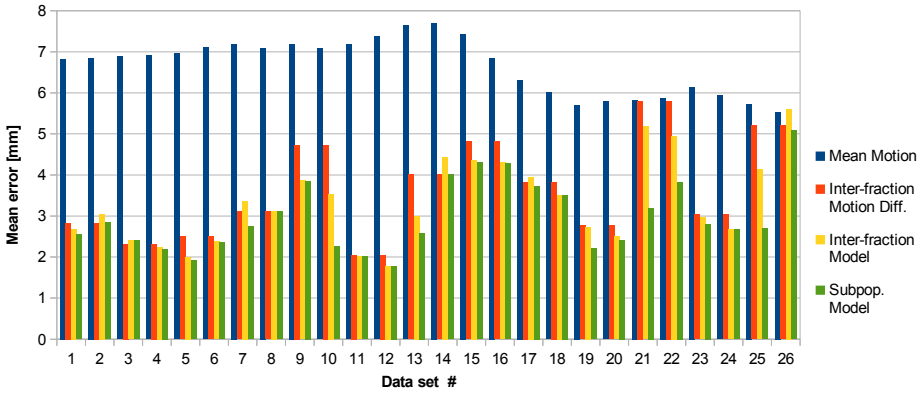

Fig. 1. Mean estimation errors of inter-fraction and subpopulation models for all 26 data sets (mean results over all 3 phases). In addition mean motion and inter-fraction motion differences are given.

for building the subpopulation models. A strong correlation (correlation coefficient of 0.85) between inter-fraction differences and mean estimation accuracy improvements achieved by the subpopulation models compared to the patient-specific inter-fraction models is observed.

4 Conclusion

Current respiratory motion compensation approaches in radiation therapy usually employ patient-specific correspondence models to relate surrogate signal measurements to internal motion patterns. In this work, an investigation on whether the motion estimation accuracy in the presence of inter-fraction motion variations can be improved by correspondence models that incorporate both patient-specific motion information obtained from a planning data set as well as motion information from selected additional patients with similar breathing motion was carried out. A sparse manifold clustering approach was employed to automatically identify subpopulations of patients with similar motion characteristics. The evaluation based on 13 patients with repeated 4D CT scans showed that these so-called subpopulation models, on average, outperform patient-specific correspondence models in the presence of inter-fraction motion variations. However, for most patients, only small differences between both models exist. Furthermore, it has to be noted that the parameter k in our clustering approach, which controls the number of patients in the chosen subpopulation, was retrospectively optimized with respect to the estimation error. Future work will therefore focus on finding ways to choose this parameter automatically. Moreover, all experiments in this work were carried out in a common atlas space. Hence, an efficient integration of this approach into a clinical workflow will be another challenge.

References

1. Keall, P.J., et al.: The management of respiratory motion in radiation oncology report of AAPM Task Group 76. Medical Physics **33**(10) (2006) 3874–3900
2. McClelland, J.: Estimating internal respiratory motion from respiratory surrogate signals using correspondence models. In: 4D Modeling and Estimation of Respiratory Motion for Radiation Therapy. Springer (2013) 187–213
3. Ehrhardt, J., Klinder, T., Lorenz, C.: Computational motion phantoms and statistical models of respiratory motion. In: 4D Modeling and Estimation of Respiratory Motion for Radiation Therapy. Springer (2013) 215 – 247
4. Wilms, M., Werner, R., Ehrhardt, J., Schmidt-Richberg, A., Schlemmer, H.P., Handels, H.: Multivariate regression approaches for surrogate-based diffeomorphic estimation of respiratory motion in radiation therapy. Physics in Medicine and Biology **59** (2014) 1147–1164
5. King, A., Buerger, C., Tsoumpas, C., Marsden, P., Schaeffter, T.: Thoracic respiratory motion estimation from MRI using a statistical model and a 2-D image navigator. Medical Image Analysis **16**(1) (2012) 252 – 264
6. McClelland, J.R., Hughes, S., Modat, M., Qureshi, A., Ahmad, S., Landau, D.B., Ourselin, S., Hawkes, D.J.: Inter-fraction variations in respiratory motion models. Physics in Medicine and Biology **56**(1) (2011) 251–272
7. Ehrhardt, J., Werner, R., Schmidt-Richberg, A., Handels, H.: Statistical Modeling of 4D Respiratory Lung Motion Using Diffeomorphic Image Registration. IEEE Trans Med Imag **30**(2) (Sep 2011) 251–65
8. Klinder, T., Lorenz, C., Ostermann, J.: Prediction framework for statistical respiratory motion modeling. Proc. MICCAI 2010 **6363** (2010) 327–334
9. Samei, G., Tanner, C., Szkely, G.: Predicting liver motion using exemplar models. In: Abdominal Imaging. Computational and Clinical Applications – 4th International Workshop at MICCAI 2012. Volume 7601 of LNCS., Springer (2012) 147–157
10. Tanner, C., Samei, G., Szekely, G.: Robust exemplar model of respiratory liver motion and individualization using an additional breath-hold image. In: Biomedical Imaging (ISBI), 2015 IEEE 12th International Symposium on. (2015) 1576 – 1579
11. Peressutti, D., Penney, G.P., Kolbitsch, C., King, A.P.: Personalising cross-population respiratory motion models using anatomical features. In: Proc. of the 17th Conference on Medical Image Understanding and Analysis. (2013) 45 – 50
12. Peressutti, D., Penney, G.P., Kolbitsch, C., King, A.P.: Personalising population-based respiratory motion models of the heart using neighbourhood approximation based on learnt anatomical features. Med Image Anal **18**(7) (2014) 1015–1025
13. Ehrhardt, J., Handels, H.: Motion Estimation in Artifact-affected 4D CT Images Using Temporal Consistent Model-based Registration with Local Adaptive Weights. In: MICCAI IGART Workshop - MICCAI 2014, Boston (2014) 5–12
14. Werner, R., Schmidt-Richberg, A., Handels, H., Ehrhardt, J.: Estimation of lung motion fields in 4D CT data by variational non-linear intensity-based registration: A comparison and evaluation study. Phys Med Biol **59** (2014) 4247–4260
15. Elhamifar, E., Vidal, R.: Sparse manifold clustering and embedding. In: Proc. NIPS. (2011) 55–63
16. Ng, A.Y., Jordan, M.I., Weiss, Y., et al.: On spectral clustering: Analysis and an algorithm. Proc. NIPS (2002) 849–856
17. Yamamoto, T., Kabus, S., von Berg, J., Lorenz, C., Chung, M.P., Hong, J.C., Loo, B.W., Keall, P.J.: Reproducibility of four-dimensional computed tomography-based lung ventilation imaging. Academic Radiology **19**(12) (2012) 1554–1565